AGU PUBLICATIONS

JGR

Journal of Geophysical Research: Biogeosciences

RESEARCH ARTICLE
10.1002/2014JG002639

Key Points:
- BrGDGTs stored in Arctic lake sediments have mixed sources
- Seasonality relates to brGDGT distribution offsets between lakes and soils
- Implications for brGDGT-based temperature proxy calibrations are assessed

Supporting Information:
- Readme
- Table S1

Correspondence to:
F. Peterse,
f.peterse@uu.nl

Citation:
Peterse, F., J. E. Vonk, R. M. Holmes, L. Giosan, N. Zimov, and T. I. Eglinton (2014), Branched glycerol dialkyl glycerol tetraethers in Arctic lake sediments: Sources and implications for paleothermometry at high latitudes, *J. Geophys. Res. Biogeosci.*, *119*, 1738–1754, doi:10.1002/2014JG002639.

Received 4 FEB 2014
Accepted 7 AUG 2014
Accepted article online 11 AUG 2014
Published online 29 AUG 2014

Branched glycerol dialkyl glycerol tetraethers in Arctic lake sediments: Sources and implications for paleothermometry at high latitudes

Francien Peterse[1,2], Jorien E. Vonk[1,2], R. Max Holmes[3], Liviu Giosan[4], Nikita Zimov[5], and Timothy I. Eglinton[1]

[1]Geological Institute, ETH Zürich, Zürich, Switzerland, [2]Now at Department of Earth Sciences, Utrecht University, Utrecht, Netherlands, [3]Woods Hole Research Center, Falmouth, Massachusetts, USA, [4]Geology and Geophysics, Woods Hole Oceanographic Institution, Woods Hole, Massachusetts, USA, [5]Pacific Institute of Geography, North-East Science Station, Far Eastern Branch of Russian Academy of Sciences, Cherskiy, Russian Federation

Abstract Branched glycerol dialkyl glycerol tetraethers (brGDGTs) are analyzed in different lakes of the Mackenzie (Canadian Arctic) and Kolyma (Siberian Arctic) River basins to evaluate their sources and the implications for brGDGT-based paleothermometry in high-latitude lakes. The comparison of brGDGT distributions and concentrations in the lakes with those in river suspended particulate matter, riverbank sediments, and permafrost material indicates that brGDGTs in Arctic lake sediments have mixed sources. In contrast to global observations, distributional offsets between brGDGTs in Arctic lakes and elsewhere in the catchment are minor, likely due to the extreme seasonality and short window of biological production at high latitudes. Consequently, both soil- and lake-calibrated brGDGT-based temperature proxies return sensible temperature estimates, even though the mean air temperature (MAT) in the Arctic is below the calibration range. The original soil-calibrated MBT-CBT (methylation of branched tetraethers–cyclisation of branched tetraethers) proxy generates MATs similar to those in the studied river basins, whereas using the recently revised MBT'-CBT calibration overestimates MAT. The application of the two global lake calibrations, generating summer air temperatures (SAT) and MAT, respectively, illustrates the influence of seasonality on the production of brGDGTs in lakes, as the latter overestimates actual MAT, whereas the SAT-based lake calibration accounts for this influence and consequently returns more accurate temperatures. Our results in principle support the application of brGDGT-based temperature proxies in high-latitude lakes in order to obtain long-term paleotemperature records for the Arctic, although the calibration and associated transfer function have to be selected with care.

1. Introduction

About half of the total amount of organic carbon (OC) stored on the continents is held in permafrost soils at high latitudes [*Tarnocai et al.*, 2009]. With Arctic regions currently warming 2 to 3 times faster than other regions [*Richter-Menge et al.*, 2011], thaw and decomposition of OC previously held in permafrost soils may release additional greenhouse gases to the atmosphere, triggering a positive feedback to global warming [*McGuire et al.*, 2009; *Schaefer et al.*, 2011]. These anticipated changes highlight the need for a better understanding of the relationships between climate, permafrost dynamics, and ecosystem adaptation, including refined estimates of past climatic variability, in order to improve our ability to make long-term predictions. However, continuous instrumental temperature records are fragmented for high latitudes and mostly only cover the past century [*Chylek et al.*, 2009; *Callaghan et al.*, 2010].

One way to reconstruct past temperatures beyond the instrumental record is through the use of paleoclimate proxies. So far, studies of tree rings and varve thicknesses have extended the Arctic paleoclimate record to the past four centuries [e.g., *Overpeck et al.*, 1997]. Recent analytical advances in the field of organic geochemistry however have enabled the reconstruction of past continental air temperature variability over much longer time scales using biomarkers. For example, the molecular distributions of a group of soil bacterial membrane lipids, the branched glycerol dialkyl glycerol tetraethers (brGDGTs; Figure 1), were found to be related to the annual mean air temperature (MAT) and soil pH of their habitat [*Weijers et al.*, 2007b]. Based on empirically derived relationships between these environmental parameters, and the number of cyclopentane moieties and methyl branches attached to the GDGT backbone, a new paleotemperature proxy

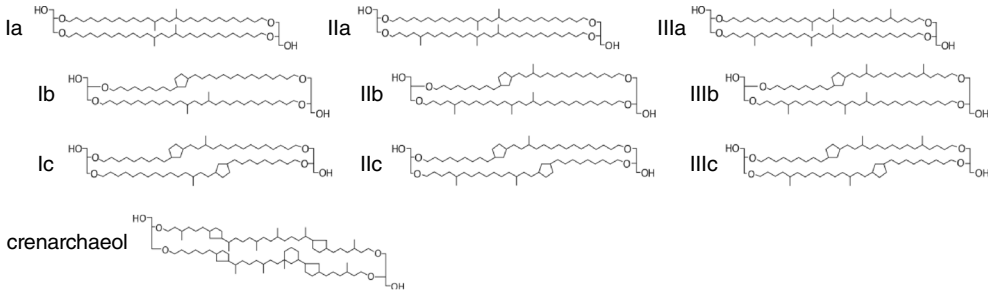

Figure 1. Molecular structures of brGDGTs and crenarchaeol.

was proposed. This so-called MBT-CBT (methylation of branched tetraethers–cyclisation of branched tetraethers) proxy [*Weijers et al.*, 2007b], recently revised as MBT′-CBT by *Peterse et al.* [2012], excluding brGDGT-IIIb and IIIc (Figure 1), has so far mainly been applied in terrestrially influenced coastal margin sediments, where brGDGTs are interpreted as an integrated climate signal of the adjacent river basin [e.g., *Weijers et al.*, 2007a; *Rueda et al.*, 2009; *Bendle et al.*, 2010], as well as in a few terrestrial archives [e.g., *Hren et al.*, 2010; *Peterse et al.*, 2011b; *Gao et al.*, 2012].

Lake sediments may also contain high-temporal-resolution archives of past terrestrial climate. Over the past few years, there have been several reconstructions of past continental air temperature based on brGDGTs in lacustrine sediments [e.g., *Fawcett et al.*, 2011; *Loomis et al.*, 2012; *Sinninghe Damsté et al.*, 2012a]. The MBT-CBT proxy is calibrated on brGDGT distributions in surface soils, so that its application in lacustrine settings depends on the assumption that brGDGTs in lake sediments are exclusively derived from soils that are delivered to the lake by erosion and subsequent runoff. However, several studies have now shown that brGDGTs in lakes may also be produced in situ [e.g., *Sinninghe Damsté et al.*, 2009; *Tierney and Russell*, 2009; *Wang et al.*, 2012; *Schoon et al.*, 2013]. The latter source of brGDGTs seems to result in a "cold" bias in the relative distribution and hence an underestimation of reconstructed MATs [e.g., *Sinninghe Damsté et al.*, 2009; *Tierney and Russell*, 2009; *Tierney et al.*, 2010; *Loomis et al.*, 2011; *Naeher et al.*, 2014].

In efforts to correct for in situ-produced brGDGTs and improve the reconstruction of paleotemperatures using brGDGTs in lacustrine settings, lake-specific proxy calibrations based on brGDGTs in surface sediments of globally distributed [*Pearson et al.*, 2011; *Sun et al.*, 2011] and tropical African lakes [*Tierney et al.*, 2010; *Loomis et al.*, 2012] have been proposed. However, the Arctic is generally underrepresented in the global lake calibration data sets, so that compared to the relatively well-studied tropical lakes, little is known about the sources and temperature sensitivity of brGDGTs in high-latitude lakes, where environmental conditions (e.g., temperature, precipitation, light availability, and ice cover) and their large seasonal variation are markedly different from in the tropics.

Here we investigated brGDGT abundances and distributions in lakes from two different high Arctic regions, the Kolyma watershed in northeastern Siberia, Russia, and the Mackenzie Delta in Northwest Territories, Canada. In addition, brGDGTs in the main sources of sediment to the lakes, i.e., river suspended particulate material (SPM), riverbank sediments, and permafrost material, were analyzed to constrain brGDGT sources. This subsequently enabled us to assess the applicability of soil- and lake-specific brGDGT calibrations on Arctic lake sediments and the reliability of resulting estimates of MAT.

2. Study Area

2.1. Siberian Arctic

Seven lakes from two distinct systems occurring in the Kolyma watershed in Russia were included in this study (Figure 2). The Kolyma River drains the Earth's largest catchment that is completely underlain with continuous permafrost (650,000 km^2 [*Holmes et al.*, 2012]). The MAT in the region varies from −11.5°C in Cherskiy, close to the river mouth and −3.2°C in Magadan, near the southernmost part of the watershed.

The lake systems can be distinguished in the way that OC is delivered to the lake; the lakes situated in the Kolyma floodplain (floodplain lakes; FP) are primarily fed by the river and receive the largest supply of organic

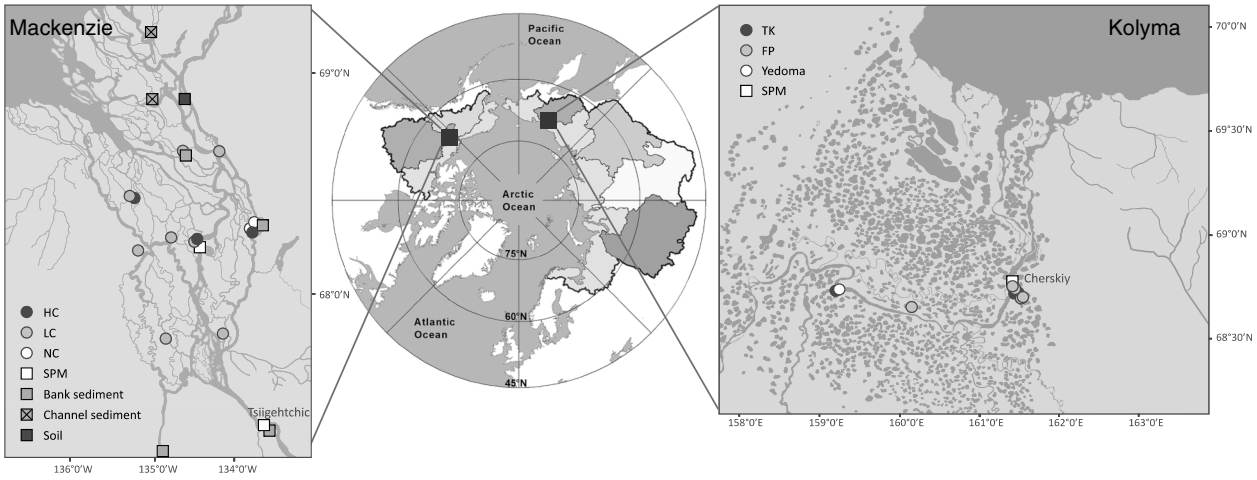

Figure 2. Overview map of Arctic river catchments with blowup maps of the Mackenzie and Kolyma River basins and sample locations. TK = thermokarst lake, FP = floodplain lake, SPM = suspended particulate material, HC = high closure lake, LC = low closure lake, and NC = no closure lake.

matter during the freshet, the brief but intense spring flood after the onset of snowmelt. Thermokarst lakes (TK) on the other hand receive no input from the river and are formed through landscape collapse following belowground ice wedge melt and permafrost thaw. Surface Holocene soils and thick yedoma deposits (~25 m [*Zimov et al.*, 2006b]) are the major suppliers of organic matter to the TK lakes. Yedoma is a relatively organic-rich late Pleistocene deposit with a high ice content that covers parts of the Siberian Arctic and Alaska and is formed by the rapid incorporation of sediments (eolian, alluvial, colluvial, and/or nival) into the permafrost [*Schirrmeister et al.*, 2011]. Yedoma underlays about 25% of the land surface in the Kolyma basin [*Zimov et al.*, 2006a].

2.2. Canadian Arctic

The 15 lakes from the Canadian Arctic included in this study are located in the delta of the Mackenzie River (Figure 2). The Mackenzie River drains a watershed of 1,780,000 km^2 [*Holmes et al.*, 2012] and is the largest supplier of fluvial sediments to the Arctic Ocean [*Holmes et al.*, 2002]. The MAT in the basin ranges from 0.7°C in the south (Fort McMurray) to −8.8°C at Inuvik in the delta. Several large lakes (notably Lake Athabasca, Great Slave Lake, and Great Bear Lake) serve as natural sediment traps along the course of the river and its tributaries, so sediment discharge to the delta is likely to be more strongly influenced by inputs downstream of these lakes. Hence, the MAT in the area of these lakes (−4.6°C at Yellowknife, on the north bank of Great Slave Lake) is more likely upper MAT end-member for this study.

All of the studied lakes receive organic material from the Mackenzie River, but their sediments and OC inflow depend on their connection time with the river. The lakes can be classified into three different groups based on the frequency and length of their connection time with the river. No closure (NC) lakes have a continuous connection with the main channel, whereas low closure (LC) lakes only flood in spring and lose their connection with the river when their water levels fall below average flood level. High closure (HC) lakes are only in contact with the river during higher-than-average floods, generally happening every 1–4 years for spring floods and >50 years for summer floods [*Marsh and Hey*, 1989].

3. Methods

3.1. Sample Collection

3.1.1. Kolyma

Lake surface sediments (Figure 2) were collected in July 2011 with a Van Veen grab sampler, subsampled, and dried overnight at 60°C at the Northeast Science Station (Cherskii, Russia). Yedoma cliff material was collected in July 2010 from Duvannyi Yar, a well-known Yedoma exposure along the Kolyma River, and stored frozen after collection. Yedoma thaw streams from the same exposure were sampled in July 2010 and July 2011 and filtered through 0.7 μm preashed GF/F filters within 24 h after collection and frozen until further

analysis. The Yedoma deposits from this exposure exhibit conventional ^{14}C ages of between 13 and 45 kyr [*Vasil'chuk and Vasil'chuk*, 1997], and corresponding ages for suspended material from the thaw streams are between 19 and 38 kyr [*Vonk et al.*, 2013]. Kolyma River SPM (Figure 2) was collected in May–July 2011 and 2012 and filtered through 0.7 μm preashed GF/F filters within 24 h after collection, except for the freshet and under-ice samples that were frozen for approximately 1 month, then thawed and filtered. All samples were collected as part of the Polaris Project (www.thepolarisproject.org).

3.1.2. Mackenzie

Sediment cores (piston cores) were collected from delta lakes (Figure 2) in March 2007 and March 2009 (L. Giosan and T. I. Eglinton, personal communication, 2014). The cores were shipped in insulated boxes (cold but unfrozen) to Woods Hole Oceanographic Institution (USA) and split lengthwise using metal cutting shears, wrapped, and put into refrigerated storage. Core tops were subsampled in February 2011. Channel sediments from Middle and Reindeer Channel of the Mackenzie River (Figure 2) were collected with a Smith–McIntyre grab sampler as part of a large sampling program in 1987 in the Mackenzie River and Beaufort Sea [*Macdonald et al.*, 1988]. Mackenzie River SPM was collected in May–June 2011 as part of the Arctic Great Rivers Observatory (www.arcticgreatrivers.org) from the East Channel near Inuvik (18 May, 27 May, and 11 June) and from the main channel near Tsiigehtchic (other dates). During the same month, freshly deposited riverbank sediments were collected after the spring flood at East Channel and Peel River. The soil sample was collected in April 2007 from a ridge out of reach from the spring freshet, close to the East Channel.

3.2. Total Organic Carbon Analysis

Freeze-dried, homogenized material was treated with 1 M HCl to remove potential carbonates prior to total organic carbon (TOC) content measurements using an elemental analyzer EA 3000 (EuroVector, Italy) at ETH Zürich.

3.3. BrGDGT Analysis

The 0.1–2.5 g freeze-dried and homogenized material was extracted with a MARSXpress microwave extraction system using dichloromethane (DCM):MeOH 9:1 (vol/vol). The total lipid extracts (TLEs) were dried under N_2. For selected samples, an aliquot was saponified with 0.5 M KOH in MEOH at 70°C for 2 h, after which Milli-Q water was added, and hexane was used to retrieve a neutral fraction. The remainder was acidified to pH = 2 with HCl, from which an acid fraction was retrieved using hexane:DCM 4:1 (vol/vol).

A known amount of C_{46} GDGT standard was added to either the neutral fraction or directly to the TLE (when not subjected to saponification). The TLEs/neutral fractions were dissolved in 9:1 (vol/vol) hexane:DCM and passed over a silica column (deactivated with Milli-Q water, 1% dry weight) to separate the extract into an apolar and a polar fraction, using 9:1 (vol/vol) hexane:DCM and 1:1 (vol/vol) DCM:MeOH, respectively. The polar fraction (containing the GDGTs) was dried under N_2, dissolved in 99:1 hexane:isopropanol, and filtered over a 0.45 μm polytetrafluorethylene filter prior to analysis with high performance liquid chromatography (LC)/atmospheric pressure chemical ionization–mass spectrometry (MS) on an Agilent 1260 Infinity series LC-MS according to *Schouten et al.* [2007]. The separation of the GDGTs was achieved with a Grace Prevail Cyano column (3 μm, 150 × 2.1 mm) after passing through a Guard column of the same material (5 μm, 7.5 × 2.1 mm) with hexane:isopropanol (99:1, vol/vol) as an eluent. Flow rate was 0.2 mL/min. Each GDGT fraction was eluted isocratically with 90% A and 10% B for 5 min, and then with a linear gradient to 18% B for 34 min, where A = hexane and B = hexane:isopropanol 9:1 (vol/vol). Selective ion monitoring of the $[M+H]^+$ was used to detect and quantify the different GDGTs, according to *Huguet et al.* [2006], except that a similar response factor was assumed for the GDGTs and the internal standard.

3.4. BrGDGT-Based Proxy Calculations

Annual mean air temperatures (MATs) were calculated according to the original soil calibration of *Weijers et al.* [2007b], using the MBT and CBT indices and the following transfer function in which roman numerals refer to structures in Figure 1:

$$\mathrm{MBT} = (\mathrm{Ia} + \mathrm{Ib} + \mathrm{Ic})/(\mathrm{Ia} + \mathrm{Ib} + \mathrm{Ic} + \mathrm{IIa} + \mathrm{IIb} + \mathrm{IIc} + \mathrm{IIIa} + \mathrm{IIIb} + \mathrm{IIIc}) \quad (1)$$

$$\mathrm{CBT} = -\log\left((\mathrm{Ib} + \mathrm{IIb})/(\mathrm{Ia} + \mathrm{IIa})\right) \quad (2)$$

$$\mathrm{MAT} = (\mathrm{MBT}–0.122–(0.187*\mathrm{CBT}))/0.02 \quad (3)$$

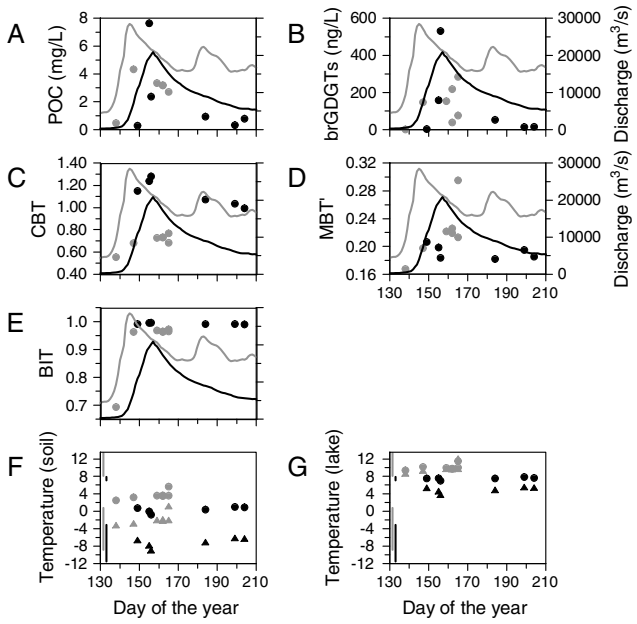

Figure 3. Amount of (a) particulate organic carbon (POC) and (b) brGDGTs transported by the Kolyma (black) and Mackenzie (grey) Rivers; (c) CBT, (d) MBT′, and (e) BIT indices for river SPM, with river discharge indicated in black (Kolyma, average 1999–2010) and grey (Mackenzie, 2011); brGDGT-derived temperatures based on the (f) soil (triangles [*Weijers et al.*, 2007b]; circles [*Peterse et al.*, 2012]) and (g) global lake calibrations (triangles [*Sun et al.*, 2011]; circles [*Pearson et al.*, 2011]) versus time. The vertical bars indicate the range of annual and summer temperatures in the catchments of the Kolyma (black) and Mackenzie (grey) Rivers.

as well as according to the revised soil calibration of *Peterse et al.* [2012], using the previously defined CBT index (equation (2)), the MBT′ index, and the newly derived transfer function:

$$\mathrm{MBT'} = (\mathrm{Ia} + \mathrm{Ib} + \mathrm{Ic})/(\mathrm{Ia} + \mathrm{Ib} + \mathrm{Ic} + \mathrm{IIa} + \mathrm{IIb} + \mathrm{IIc} + \mathrm{IIIa}) \quad (4)$$

$$\mathrm{MAT'} = 0.81\text{–}5.67\text{*CBT} + 31.0\text{*MBT'} \quad (5)$$

The MAT was also calculated based on the lake-specific calibration of *Sun et al.* [2011], who use the MBT and CBT indices (equations (1) and (2)) and the following function for worldwide application for lakes with pH < 8.5:

$$\mathrm{MAT} = 6.803\text{–}7.062\text{*CBT} + 37.09\text{*MBT} \quad (6)$$

Finally, the global lake calibration of *Pearson et al.* [2011] was applied to derive mean summer air temperatures (SATs) based on the fractional abundance of a selection of brGDGTs:

$$\mathrm{SAT} = 20.9 + 98.1\text{*}f(\mathrm{Ib})\text{–}12.0\text{*}f(\mathrm{IIa})\text{–}20.5\text{*}f(\mathrm{IIIa}) \quad (7)$$

The branched and isoprenoid tetraether (BIT) index was calculated according to *Hopmans et al.* [2004]:

$$\mathrm{BIT} = (\mathrm{Ia} + \mathrm{IIa} + \mathrm{IIIa})/(\mathrm{Ia} + \mathrm{IIa} + \mathrm{IIIa} + \mathrm{crenarchaeol}) \quad (8)$$

3.5. Statistical Analysis

The significance of differences between the GDGT concentrations and the GDGT-based index values for each sample set was tested using the distribution-independent bootstrapping method [cf. *Efron*, 1979]. In short, each data set of *n* observations was resampled (or bootstrapped) by sampling with replacement to form a new sample that is also of size *n*, using MetaWin 2.1. This process was repeated 5000 times for each sample set, after which the mean was computed. Average values were considered significantly different if their 95% confidence interval did not overlap. Significantly different groups are indicated with a letter.

Table 1. Sampling Date, Coordinates, and Total Organic Carbon (TOC) Content for the Lakes, SPM, Yedoma, Soil, and Riverbank Sediments in the Kolyma and Mackenzie River Basins

Sample Type	Sample Name/ Location	Sample Date	Latitude (°N)	Longitude (°E)	TOC (% or mg/L)
Kolyma Region, Northeast Siberia, Russia					
Thermokarst lake	Tube Dispenser Lake	11 July 2011	68.765	161.402	4.8
Thermokarst lake	Duvannyi Yar Lake	13 July 2011	68.628	159.147	20.8
Thermokarst lake	Shuchi Lake	7 July 2011	68.746	161.393	22.6
Floodplain lake	Fire Lake	10 July 2011	68.719	161.451	6.2
Floodplain lake	Pantaleikha Lake	8 July 2011	68.734	161.446	2.0
Floodplain lake	Airport 33 Lake	15 July 2011	68.736	161.329	4.1
Floodplain lake	Airport 34 Lake	18 July 2011	68.733	161.332	2.3
Floodplain lake	Leonid Lake	12 July 2011	68.579	160.090	4.2
Yedoma	Duvannyi Yar cliff	27 July 2010	68.631	159.151	1.7
Yedoma stream[a]	Duvannyi Yar stream A	27 July 2010	68.631	159.150	8580
Yedoma stream[a]	Duvannyi Yar stream B	27 July 2010	68.631	159.148	8480
Yedoma stream[a]	Duvannyi Yar stream C	27 July 2010	68.631	159.126	9240
Yedoma stream[a]	Duvannyi Yar stream D	27 July 2010	68.631	159.122	6700
Yedoma stream	Duvannyi Yar stream 3	22 July 2011	68.631	159.150	-
Yedoma stream	Duvannyi Yar stream 4	22 July 2011	68.631	159.148	-
Yedoma stream	Duvannyi Yar stream 5	22 July 2011	68.631	159.126	-
Yedoma stream	Duvannyi Yar stream 6	22 July 2011	68.631	159.122	-
SPM under ice[a]	Kolyma River	29 May 2011	68.734	161.387	0.3
SPM freshet[a]	Kolyma River	4 June 2011	68.734	161.387	7.6
SPM freshet[a]	Kolyma River	5 June 2012	68.734	161.387	2.4
SPM low flow[a]	Kolyma River	3 July 2012	68.734	161.387	0.9
SPM low flow[a]	Kolyma River	18 July 2012	68.734	161.387	0.3
SPM low flow[a]	Kolyma River	23 July 2011	68.734	161.387	0.8
Mackenzie Delta, Northwest Territories, Canada					
No closure	MD-2	March 2009	68.4	−133.8	1.6
No closure	MD-4	March 2009	68.3	−133.9	1.9
No closure	MD-6	March 2009	68.3	−133.9	1.6
Low closure	LD-1	March 2007	68.7	−134.6	1.2
Low closure	MD-10	March 2009	68.3	−134.8	1.8
Low closure	LD-2	March 2009	68.7	−134.2	3.5
Low closure	MD-12	March 2009	68.2	−135.1	4.8
Low closure	UD-1	March 2009	67.9	−134.8	2.8
Low closure	UD-3	March 2009	67.9	−134.2	2.5
Low closure	UD-4	March 2009	67.9	−134.2	1.6
Low closure	MD-8	March 2009	68.3	−134.5	1.3
Low closure	LD-3	March 2009	68.5	−135.2	1.5
High closure	MD-8	March 2009	68.3	−134.5	3.2
High closure	LD-4	March 2009	68.5	−135.3	2.6
High closure	MD-5	March 2009	68.3	−133.8	5.7
Riverbank sediment	East Channel	31 May 2011	68.3	−133.7	1.9
Channel sediment	Middle Channel	June 1987	69.2	−135.0	1.1
Channel sediment	Reindeer Channel	July 1987	68.9	−135.0	1.5
Riverbank sediment	Peel River	5 June 2011	67.3	−134.9	0.8
Riverbank sediment	Tsiigehtchic	8 June 2011	67.5	−133.7	3.3
Levee sediment	Lake LD-1	March 1994	68.7	−134.5	0.9
Surface soil	Mackenzie soil	April 2007	68.9	−134.6	1.3
SPM under ice[a]	Mackenzie River	18 May 2011	67.45	−133.76	0.5
SPM freshet[a]	Mackenzie River	27 May 2011	67.45	−133.76	4.3
SPM low flow[a]	Mackenzie River	8 June 2011	67.45	−133.76	3.4
SPM low flow[a]	Mackenzie River	11 June 2011	67.45	−133.76	3.2
SPM low flow[a]	Mackenzie River	11 June 2011	67.45	−133.76	3.2
SPM low flow[a]	Mackenzie River (middle channel)	14 June 2011	68.25	−134.39	-
SPM low flow[a]	Mackenzie River (Tsiigehtchic)	14 June 2011	67.45	−133.76	2.7

[a]TOC content in mg/L.

Journal of Geophysical Research: Biogeosciences 10.1002/2014JG002639

Table 2. BrGDGT Concentrations, Index Values, and Proxy-Derived Temperatures for the Lake Sediments, SPM, Yedoma, Soil, and Riverbank Sediments in the Kolyma and Mackenzie River Basins

Sample Type	Sample Name/ Location	brGDGTs (ng/g Dry Weight Sediment or L)	brGDGTs (μg/g TOC)	BIT (Equation (8))	CBT (Equation (2))	MBT (Equation (1))	MBT (Equation (4))	MAT [*Weijers et al.*, 2007b]	MAT′ [*Peterse et al.*, 2012]	MAT [*Sun et al.*, 2011]	SAT [*Pearson et al.*, 2011]
Kolyma Region, Northeast Siberia, Russia											
Thermokarst lake	Tube Dispenser Lake	7,037	146	1.00	1.15	0.19	0.19	−7.3	0.2	4.8	5.9
Thermokarst lake	Duvannyi Yar Lake	39,269	189	1.00	0.93	0.15	0.15	−7.6	0.0	4.3	5.3
Thermokarst lake	Shuchi Lake	47,676	211	1.00	1.15	0.19	0.19	−7.2	0.3	4.9	6.1
Floodplain lake	Fire Lake	8,836	144	1.00	1.09	0.15	0.15	−8.6	-0.6	4.3	5.7
Floodplain lake	Pantaleikha Lake	4,805	245	1.00	1.05	0.19	0.19	−6.4	0.8	5.3	8.5
Floodplain lake	Airport 33 Lake	11,191	276	1.00	0.91	0.15	0.15	−7.3	0.2	4.4	6.6
Floodplain lake	Airport 34 Lake	4,469	194	1.00	1.00	0.15	0.15	−8.0	-0.2	4.1	6.4
Floodplain lake	Leonid Lake	12,046	284	1.00	0.86	0.14	0.14	−7.4	0.2	4.3	6.3
Yedoma	Duvannyi Yar cliff	161	9.2	0.82	0.39	0.15	0.15	−2.1	3.4	7.6	13.5
Yedoma stream[a]	Duvannyi Yar stream A	167	1.9	0.83	0.77	0.24	0.24	−1.3	3.9	8.8	11.8
Yedoma stream[a]	Duvannyi Yar stream B	30	0.4	0.89	0.71	0.20	0.20	−2.9	2.9	7.5	10.5
Yedoma stream[a]	Duvannyi Yar stream C	64	0.8	0.81	1.01	0.24	0.24	−3.5	2.5	7.5	8.1
Yedoma stream[a]	Duvannyi Yar stream D	60	0.9	0.82	1.00	0.23	0.23	−3.9	2.3	7.2	8.0
Yedoma stream[a]	Duvannyi Yar stream 3	55	-	0.83	0.96	0.21	0.21	−4.3	2.1	6.8	8.2
Yedoma stream[a]	Duvannyi Yar stream 4	55	-	0.84	1.14	0.23	0.23	−5.3	1.4	6.3	10.8
Yedoma stream[a]	Duvannyi Yar stream 5	41	-	0.82	0.88	0.21	0.21	−3.9	2.3	7.0	8.7
Yedoma stream[a]	Duvannyi Yar stream 6	61	-	0.83	0.95	0.21	0.21	−4.5	1.9	6.6	8.2
SPM under ice	Kolyma River 29 May 2011	2	0.8	0.99	1.15	0.21	0.21	−6.6	0.7	5.4	7.5
SPM freshet[a]	Kolyma River 4 June 2011	159	2.1	1.00	1.24	0.20	0.20	−7.8	-0.1	4.6	7.5
SPM freshet	Kolyma River 4 June 2012	531	22.1	1.00	1.28	0.18	0.18	−8.9	-0.8	3.8	7.0
SPM low flow	Kolyma River 3 July 2012	52	5.8	0.99	1.07	0.18	0.18	−7.0	0.4	4.9	7.5
SPM low flow	Kolyma River 18 July 2012	14	4.6	0.99	1.04	0.19	0.19	−6.1	1.0	5.6	7.8
SPM low flow	Kolyma River 23 July 2011	15	1.9	0.99	0.99	0.18	0.18	−6.2	0.9	5.4	7.6
Mackenzie Delta, Northwest Territories, Canada											
No closure	MD-2	3,438	211	0.94	0.62	0.25	0.25	0.4	5.1	9.9	12.9
No closure	MD-4	6,146	327	0.98	0.54	0.17	0.17	−2.7	3.1	7.4	9.0
No closure	MD-6	3,056	186	0.97	0.56	0.17	0.18	−2.6	3.2	7.5	11.2
Low closure	LD-1	336	28	0.95	0.57	0.21	0.21	−1.2	4.1	8.6	11.2
Low closure	MD-10	3,018	170	0.97	0.61	0.15	0.15	−4.5	2.0	6.1	8.7
Low closure	LD-2	8,201	237	0.99	0.94	0.11	0.11	−9.5	-1.1	2.8	7.9
Low closure	MD-12	16,008	335	1.00	0.65	0.11	0.11	−6.8	0.5	4.4	7.3
Low closure	UD-1	4,731	208	0.99	0.54	0.14	0.14	−4.3	2.1	6.2	9.3
Low closure	UD-3	6,422	254	0.99	0.67	0.14	0.15	−5.3	1.5	5.6	10.5
Low closure	UD-4	2,587	159	0.98	0.67	0.15	0.16	−4.6	2.1	6.1	9.9
Low closure	MD-8	12,147	949	1.00	0.87	0.11	0.11	−8.8	-0.7	3.2	7.1
Low closure	LD-3	2,776	245	0.99	0.61	0.13	0.14	−5.2	1.6	5.6	11.3
High closure	MD-8	3,837	121	0.99	0.49	0.16	0.16	−2.8	3.0	7.2	12.3
High closure	LD-4	5,250	206	0.99	0.65	0.13	0.13	−5.6	1.3	5.4	10.2
High closure	MD-5	22,757	399	1.00	0.56	0.13	0.15	−4.8	2.4	5.8	11.3
Riverbank sediment	East Channel	294	294	0.98	0.57	0.20	0.20	−1.5	3.8	8.3	11.0
Channel sediment	Middle Channel	371	371	0.98	0.61	0.22	0.23	−0.6	4.4	9.1	11.9
Channel sediment	Reindeer Channel	512	512	0.98	0.61	0.22	0.22	−1.0	4.2	8.8	11.6
Riverbank sediment	Peel River	99	99	0.99	0.61	0.31	0.31	3.5	7.0	12.2	13.9
Riverbank sediment	Tsiigehtchic	711	711	0.97	0.68	0.23	0.24	−0.7	4.4	9.1	12.1
Levee sediment	Lake LD-1	302	302	0.97	0.57	0.21	0.22	−0.7	4.4	8.9	12.0
Surface soil	Mackenzie Soil	-	-	0.99	0.85	0.19	0.19	−4.6	1.9	6.4	8.2
SPM under ice	Mackenzie River 18 May 2011	2	0.3	0.69	0.55	0.16	0.17	−3.2	2.9	7.0	9.0

Table 2. (continued)

Sample Type	Sample Name/ Location	brGDGTs (ng/g Dry Weight Sediment or L)	brGDGTs (μg/g TOC)	BIT (Equation (8))	CBT (Equation (2))	MBT (Equation (1))	MBT (Equation (4))	MAT [*Weijers et al.*, 2007b]	MAT′ [*Peterse et al.*, 2012]	MAT [*Sun et al.*, 2011]	SAT [*Pearson et al.*, 2011]
SPM freshet	Mackenzie River 27 May 2011	33	0.8	0.96	0.68	0.19	0.20	−2.8	3.1	7.5	9.9
SPM low flow	Mackenzie River 8 June 2011	46	1.3	0.97	0.73	0.22	0.22	−2.0	3.6	8.2	9.7
SPM low flow	Mackenzie River 11 June 2011	12	0.4	0.96	0.73	0.22	0.23	−1.9	3.7	8.3	9.7
SPM low flow	Mackenzie River 11 June 2011	69	2.1	0.96	0.73	0.22	0.22	−2.1	3.5	8.1	9.5
SPM low flow	Mackenzie River 14 June 2011	-	-	0.96	0.68	0.21	0.21	−2.0	3.5	8.1	9.7
SPM low flow	Mackenzie River 14 June 2011	105	3.9	0.97	0.77	0.29	0.30	1.2	5.6	10.7	11.3

[a]TOC content in mg/L.

4. Results

4.1. Total Organic Carbon

4.1.1. Kolyma

The concentration of particulate organic carbon (POC) in river SPM varied between 0.28 mg/L in late May, when the river was ice covered, and 2.37–7.64 mg/L in early June, during the peak of the freshets in 2011 and 2012 (Figure 3), whereas that in the yedoma streams is 3 orders of magnitude higher (6700–9240 mg/L). The TOC concentration in the lake surface sediments is higher in the TK lakes than in the FP lakes and varies between 4.8–22.6% and 2.0–6.2%, respectively (Table 1).

4.1.2. Mackenzie

POC in the Mackenzie River varied between 0.5 mg/L under ice and reached 4.3 mg/L during the freshet in 2011 (Figure 3). Bank, channel, and levee deposits contain 0.8–3.3% TOC. The concentration of TOC in the sediment of the different lake types increases with a decrease in river contact and is 1.7 ± 0.1% ($n = 3$) in the NC lakes, 2.3 ± 1.2% ($n = 9$) in the LC lakes, and 3.8 ± 1.7% ($n = 3$) in the HC lakes. The one soil sample contains 1.3% TOC (Table 1).

4.2. GDGT Concentrations

4.2.1. Kolyma

BrGDGT concentrations transported by the river follow the trend of POC and are lowest under ice and highest during the freshet (2–531 ng/L; Table 2 and Figure 3). The concentration of brGDGTs in the lake surface sediments is quite variable (4.5–47.7 μg brGDGTs/g dry weight sediment; Table 2) but is up to an order of magnitude higher in the TK lakes than in the FP lakes. However, OC-normalized brGDGT concentrations in both lake types are not significantly different (182 ± 33 and 229 ± 59 μg/g TOC for the TK and FP lakes, respectively; Table 2 and Figure 4). Compared to the lake sediments, the yedoma streams contain very low concentrations of brGDGTs (0.03–0.2 μg/g dry weight yedoma), especially when normalized to TOC (0.4–9.2 μg/g TOC; Table 2).

4.2.2. Mackenzie

The concentration of brGDGTs in the SPM of the Mackenzie River varies between 2 and 105 ng/L and is lowest under ice (Table 2; Figure 3). In contrast to the brGDGT concentrations in SPM transported by the Kolyma River, brGDGTs in Mackenzie SPM do not show the same trend as POC. The abundance of brGDGTs in the lake surface sediments varies widely among the lakes (0.3–22.8 μg/g dry weight sediment; Table 2) but does not show a clear relation with lake type. BrGDGT concentrations are all in the same range when normalized to TOC (Table 2 and Figure 4). The amount of brGDGTs in the soil was not quantified, but riverbank, channel, and levee deposits contain 0.1–0.7 μg brGDGTs/g dry weight sediment (Table 2). The lowest concentrations are found in bank sediments from Peel River, which drains a different watershed than the Mackenzie.

4.3. GDGT Distributions

4.3.1. Kolyma

The lake surface sediments are generally dominated by brGDGT-III, whereas SPM and yedoma have a larger relative contribution of brGDGT-II (Figure 5). The MBT′, CBT, and BIT index values for the

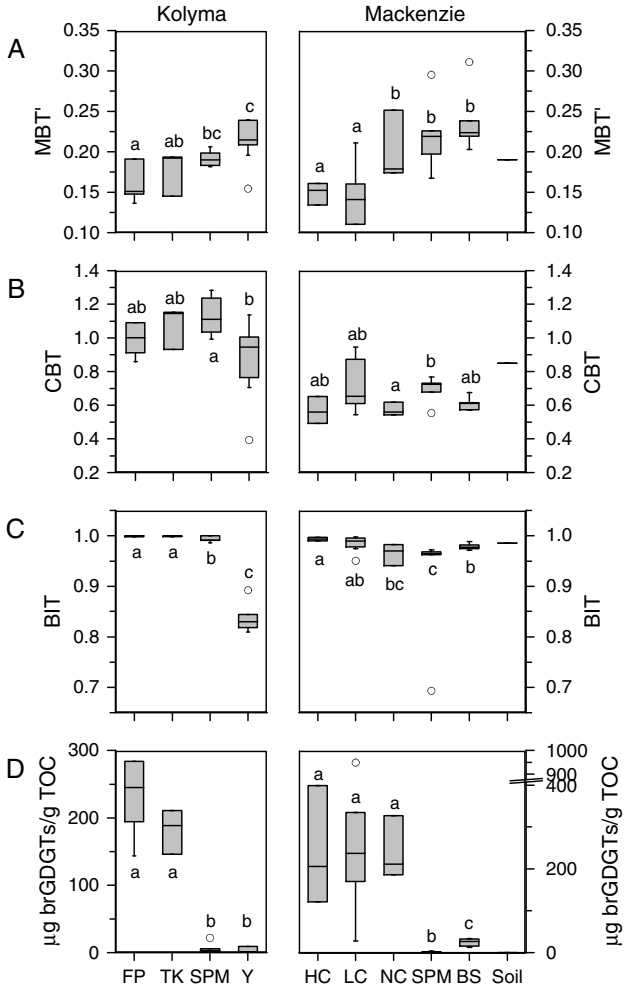

Figure 4. Box plots of (a) MBT′, (b) CBT, (c) BIT indices, and (d) TOC-normalized brGDGT concentrations for the different lake systems and potential brGDGT sources for the Kolyma and Mackenzie Rivers. The letters indicate the significant differences with 95% confidence interval. HC = high closure, LC = low closure, NC = no closure, SPM = suspended particulate material, BS = bank sediment, FP = floodplain lake, TK = thermokarst lake, and Y = yedoma.

different sample pools are given in Figure 4, in which letters indicate significant differences between the pools. The absence of significant differences in GDGT-based index values for the FP and TK lake sediments indicates similar distributions in both lake types. The GDGT distribution in the SPM transported by the Kolyma River is similar to that in the TK lakes but slightly differs from that in the FP lakes based on the significant offset in MBT′ index values between these sample sets (Figure 4). The distribution of GDGTs in yedoma is different from that in lakes based on the MBT′ index and different from that in the SPM based on the CBT index. The distinct GDGT distribution is confirmed by the BIT index values for yedoma, which are significantly lower than those in lake sediments and SPM (Figure 4).

4.3.2. Mackenzie

BrGDGTs of type II and III are most abundant in the sediments of the Mackenzie Delta lakes included in this study (Figure 5). All river SPM and bank sediments contain most of brGDGT-II, except for the SPM sampled under ice, which is dominated by brGDGT-III. The relative distribution of the brGDGTs is generally similar among the NC, LC, and HC lake types, albeit that NC lakes have slightly but significantly different MBT′ index values (Figure 4). The MBT′ index values for the NC lakes (0.20 ± 0.04) are higher than those for the LC (0.14 ± 0.03) and HC lakes (0.14 ± 0.01) but similar to river SPM (0.22 ± 0.04) and bank sediments (0.24 ± 0.04). In contrast, CBT index values do not show significant differences between lake types and bank sediments, but the CBT for river SPM only corresponds with that in the HC and LC lake sediments (Figure 4). Although bootstrapping indicates that the BIT index is significantly different between sample pools within a 95% confidence interval, the index yields high values for all samples (0.94–1.00). The only sample with a clearly distinct BIT value is the SPM collected under ice, for which the BIT index is 0.69 (Table 2 and Figure 4).

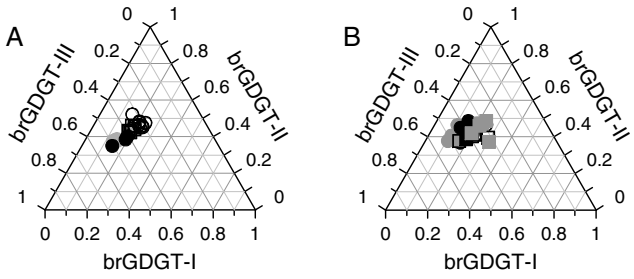

Figure 5. Triplots indicting relative distributions of brGDGTs in sample sets from the (a) Kolyma River and (b) Mackenzie River. The symbols correspond to those in Figure 2.

5. Discussion

5.1. Presence of brGDGTs in Arctic Lake Surface Sediments

5.1.1. Kolyma

The general dominance of types II and III brGDGTs in the samples from the Kolyma basin is in agreement with brGDGT

distributions in high-latitude soils from the global soil calibration set [*Weijers et al.*, 2007b; *Peterse et al.*, 2012] and with those recently reported for lake sediments from Baffin Island [*Shanahan et al.*, 2013]. The concentrations of brGDGTs are substantially different in the TK and FP lake sediments and are higher in the TK lakes (Table 2), which may be a result of the generally anoxic conditions in the lower water column of these particular lakes (e.g., dissolved $O_2 < 1$ mg/L in Shuchi and Tube Dispenser Lake at depths >5 m; $n = 10$, July 2011 and 2012, www.thepolarisproject.org/data/). BrGDGTs generally appear to be preferentially produced in anoxic environments, as, for example, has been observed in peat bogs, where not only the absolute amount of brGDGTs but also the fraction of their living, intact precursor lipids (i.e., retaining the polar head group) increases in anoxic zone below the water table [*Weijers et al.*, 2009; *Liu et al.*, 2010; *Peterse et al.*, 2011a]. However, the TOC content in the TK lakes is also considerably higher than in the FP lakes, so that brGDGT concentrations fall within the same order of magnitude for all lakes when normalized against TOC (Table 2 and Figure 4), suggesting that the higher absolute brGDGT concentrations in the TK lakes may be a preservational feature. Additionally, the Kolyma River may be responsible for the delivery of additional siliciclastic material to the FP lakes, contributing to the lower TOC content in these lakes compared to that in the TK lakes. Nevertheless, the dilution of TOC by a varying input of siliciclastic material is unrelated to the relative distribution of the brGDGTs. Hence, the coupling of brGDGT concentration and TOC content, in combination with similar relative distributions between lake types, suggests that the majority of brGDGTs in the lake sediments is likely derived from the same source.

5.1.2. Mackenzie

The dominance of type II and III brGDGTs in the Mackenzie Delta lakes fits with the results from the Kolyma basin. The distribution of brGDGTs is generally similar among the lakes, except for the NC lakes, which have slightly higher MBT′ index values. Since these lakes are in continuous connection with the river, this suggests that the duration of river contact may influence the brGDGT distribution in the underlying sediment. In contrast, the amount of brGDGTs preserved in the lake sediments does not seem to be influenced by river contact, as their abundance varies widely among the lakes, and is not directly related to lake type (Table 2). Also, TOC-normalized brGDGT concentrations are not significantly different between lake types (Figure 4). Like in the Kolyma basin, the amount of brGDGTs in the lake sediments correlates with TOC content ($r^2 = 0.67$), suggesting that a large part of the brGDGTs and the OC in lake sediments share a common source.

5.2. Constraining the Sources of brGDGTs in Arctic Lakes

5.2.1. Kolyma

The largest contribution of particulate OC to the lakes is the Kolyma floodplain is delivered by the river. This is especially true during the freshet, when the discharge and sediment load of the river reach their maximum, enabling the inflow of river water into the FP lakes through connecting channels or overbank flooding. The concentration of brGDGTs in the Kolyma SPM varies with that of the POC (Figure 3), indicating that brGDGTs are part of the SPM-associated OC. It has been shown that the major part of river SPM-associated OC is generally derived from soils [e.g., *Hedges et al.*, 1986], and this has been confirmed for the Kolyma River based on the occurrence, distribution, and isotopic composition of terrestrial biomarkers in the SPM [*Lobbes et al.*, 2000; *van Dongen et al.*, 2008]. This would suggest that also the brGDGTs in the SPM transported by the Kolyma River are mainly of soil origin, although recent studies have indicated that additional brGDGT production may take place in rivers [e.g., *Kim et al.*, 2012; *Zell et al.*, 2013; *De Jonge et al.*, 2014]. Also, the generally invariant relative distribution of SPM-associated brGDGTs would support a primary soil origin of the brGDGTs, although CBT values show a slight decrease over the sampling period (Figure 3). The limited distributional variability may be expected given (i) the relatively short period of sampling (approximately 2 months in summer) and (ii) that the watershed is uniformly underlain by permafrost soils. The similarity in MBT′ and CBT index values for the SPM and the FP lake sediments would thus support that the brGDGTs in these lakes are primarily soil derived. Also, TK lakes receive their largest part of OC from thawing permafrost soils and yedoma surrounding the lakes. Indeed, brGDGTs in the TK lakes bear the same signature as those in the river SPM and FP lakes (Figure 4), although the TK lakes are not in direct contact with the river. Hence, the brGDGT distribution in the thawing permafrost soils that directly supply brGDGTs to the TK lakes must be similar to those indirectly supplying the FP lakes after river transport.

A potential end-member for permafrost-derived brGDGTs is provided by yedoma, where the distribution of brGDGTs should reflect the environmental conditions at the time of deposition and subsequent freezing

during the late Pleistocene rather than a modern climate signal. Yedoma indeed has a distinct brGDGT signature and is characterized by a slightly higher relative contribution of type I brGDGTs, which may serve as a tracer of yedoma-derived brGDGT inputs in lakes. Although CBT index values are not significantly different for yedoma and lake sediments, the MBT′ index is (Figure 4). However, the absolute difference between the lowest lake MBT′ index value and the highest yedoma MBT′ index value is only 0.10. This is similar to the natural annual variation in MBT index values found in some midlatitude soils [*Weijers et al.*, 2011], implying that the difference in MBT′ between lakes and yedoma should not be overinterpreted, limiting the ability to assess yedoma-derived brGDGTs to the total brGDGTs pool in the lakes solely based on their distribution. Regardless of the (dis)similarities in yedoma and lake sedimentary brGDGT distributions, the concentration of brGDGTs in yedoma is so low that the signal is hard to detect in lake sediments. Hence, we conclude that thawing Holocene surface soils represent the largest source of brGDGTs supplied to the lakes. Radiocarbon measurements on brGDGTs in the lake sediments may help to resolve this issue in the future [cf. *Birkholz et al.*, 2013].

Another indication of limited yedoma input is provided by the presence of crenarchaeol (Figure 1) in yedoma, whereas this is virtually absent in the lake sediments (Table 2). Crenarchaeol is an isoprenoid GDGT that is commonly produced by marine planktonic archaea. Although it has recently also been detected in the membranes of soil Thaumarchaeota [*Sinninghe Damsté et al.*, 2012b], it normally dominates over brGDGTs in a marine environment. As a result, the branched and isoprenoid tetraethers (BIT) index has been proposed as a proxy for the relative input of soil OC to an aquatic system [*Hopmans et al.*, 2004]. Soils typically have high (>0.8) BIT index values [e.g., *Weijers et al.*, 2006; *Peterse et al.*, 2009; *Tierney and Russell*, 2009; *Schouten et al.*, 2013], although low soil BIT index values caused by increased crenarchaeol concentrations have recently been linked to aridity [e.g., *Dirghangi et al.*, 2013]. BIT index values in lakes can be quite variable [e.g., *Blaga et al.*, 2010; *Pearson et al.*, 2011] and appear to reflect variations in the concentration of crenarchaeol rather than the relative input of soil OC [e.g., *Tierney et al.*, 2010; *Pearson et al.*, 2011]. BIT index values for yedoma range from 0.81 to 0.89, whereas all lake sediments have a BIT value of 1.00, confirming the minimal contribution of yedoma-derived GDGTs to the lake sediments. Although yedoma makes up for about 25% of the soil in this area [*Zimov et al.*, 2006a], even its GDGT contribution to the river SPM is barely detectable despite similar TOC-normalized brGDGT concentrations (Figure 4).

Since the concentration and signature of brGDGTs in Holocene permafrost soils is unknown, it is not possible to confirm soils as exclusive source of brGDGTs in the lake sediments. Moreover, a growing number of studies indicate that a substantial part of brGDGTs stored in lake sediments is actually produced in situ, causing a substantial offset in MBT and CBT index values [e.g., *Tierney and Russell*, 2009; *Sinninghe Damsté et al.*, 2009; *Tierney et al.*, 2010]. Any contribution from in situ production of brGDGTs in the Kolyma lakes should thus become visible in offsets between brGDGT distributions in the lakes and the river SPM. Subsequent comparison of brGDGT-based index values for the different sample sets indicates that distributional variations in the Kolyma system are only minor and not systematic (Figure 4), suggesting limited in situ production. Nevertheless, the TOC-normalized concentration of brGDGTs in the lake sediments is 1–3 orders of magnitude higher than in SPM and yedoma (Table 2), which implies that the lakes should receive unrealistic amounts of SPM and permafrost material in order to reach the detected brGDGT concentrations in the lake sediments. This offset in brGDGT concentrations can consequently only be explained by a contribution of in situ production of brGDGTs. Interestingly, this would mean that brGDGTs in Siberian Arctic lakes are produced with a near identical distribution to that in soils, which is in contrast with what has been reported so far.

5.2.2. Mackenzie

All the Mackenzie Delta lakes included in this study receive river SPM from the Mackenzie River, but the amount decreases from the NC to the LC and HC lakes. BrGDGTs are presumably mainly supplied to the lake by freshet SPM, but additional sources should become visible by comparing their relative distribution in the different lake types and that in the SPM.

As for the Kolyma River, the freshet is the period of highest discharge and sediment load, although the peak in brGDGT concentration is slightly delayed (Figure 3). The SPM collected under ice (18 May 2011) clearly stands out with a low concentration of brGDGTs, likely reflecting base flow conditions. Its more "aquatic" BIT index value of 0.69 differentiates it from the presumably soil-influenced freshet SPM with BIT index values of 0.97 ± 0.00 (Figure 3). The distinct under-ice brGDGT signature may originate from the large and deep lake that is the main source of the Mackenzie River (Great Slave Lake; 27,200 km^2) and thus an important supplier of the base flow. This change in source is also reflected in the distribution of brGDGTs, as the MBT′ index

increases from 0.17 under ice to 0.30 later in the year, and the CBT index from 0.55 under ice to 0.77. The distribution changes during the period of sampling may be a result of a contribution of sediments flushed from flooded lakes upstream. Additionally, a varying contribution of river-produced brGDGTs may influence the composition of SPM-associated brGDGTs. Nevertheless, the most important difference is observed between under ice and (post)freshet conditions, likely representing the aquatic base flow signal and a more soil influenced signal, respectively. Similarly, *De Jonge et al.* [2014] found that the low concentrations of brGDGTs in SPM from the Yenisei River collected 2–3 months after the freshet did not match the signature of the brGDGTs in catchment soils but more likely represented a base flow signal instead. The low concentration of brGDGTs in Mackenzie under ice/base flow SPM compared to during and after the freshet suggests that the distributions of brGDGTs in the lake sediments should predominantly reflect the freshet signal. Any riverine overprint would only be expected in the NC lake sediments, since these lakes are in continuous contact with the river. Indeed, the BIT index is slightly but significantly lower in these lakes compared to the LC and HC lakes. Also, the MBT′ index for the NC lake sediments is more similar to that of the SPM and the bank sediments than those for the lake sediments exclusively receiving SPM during the freshet (Figure 4).

The distribution of brGDGTs in the LC and HC lakes results in the same CBT index values as those of the SPM and bank sediments, while MBT′ index values are significantly lower (Figure 4). Although the difference in MBT′ between these lake sediments and the river SPM is small (0.08–0.10), the offset may be introduced by a combination of additional in situ production in the LC and HC lakes and the absence of the base flow contribution as received by the NC lakes. Indeed, Mackenzie Delta lakes with shorter river-connection times (i.e., LC and HC lakes) are typically less turbid and hence have a higher autochthonous production [*Tank et al.*, 2011]. The brGDGT distributions in these lakes are characterized by a higher relative abundance of brGDGT-IIIa, which fits with the trend found in lakes worldwide [e.g., *Blaga et al.*, 2010; *Tierney et al.*, 2010; *Pearson et al.*, 2011; *Sun et al.*, 2011] and suggests that the freshet signal in these lakes is altered by additional in situ production. The one available soil sample from the Mackenzie Delta has MBT′ and CBT index values that fit in the range of those of the SPM and lake sediments and would confirm their primarily soil origin in these samples. However, due to the heterogeneity of soils [*Weijers et al.*, 2007b; *Peterse et al.*, 2012] and the natural variability in brGDGT distribution in surface soils on a small spatial scale or within a lake catchment [*Naeher et al.*, 2014; *Niemann et al.*, 2012], it is not appropriate to use this single sample as a soil end-ember.

Even though in situ brGDGT production appears to take place in those lakes with less river contact, the differences with brGDGT-based index values for river SPM and bank sediments, representing catchment soil-derived brGDGTs, are surprisingly small. The MBT′ offset is about 0.08 on average, and CBT index values even show no significant differences (Figure 4), which results in a spread in reconstructed temperatures that falls within the calibration error (5.0°C for the MBT′-CBT soil calibration of *Peterse et al.* [2012] and 2.0°C for the lake calibration of *Pearson et al.* [2011]). Hence, purely focusing on distribution data would lead to the conclusion that the proportion of brGDGTs from in situ production is minor relative to those derived from soils. However, absolute concentrations of brGDGTs in the lakes are substantially higher than in the river SPM and bank sediments (Figure 4), arguing for an important additional input of in situ produced brGDGTs not only in the LC and HC lakes but also in the NC lakes that are in continuous contact with the river. As observed for the lakes in the Kolyma basin, this implies that the lacustrine brGDGTs are produced in near similar distributions as in the catchment soils.

5.3. Influence of Seasonality on brGDGT Production in Lakes

The minor distributional differences in which brGDGTs are produced in aquatic and terrestrial environments in the Kolyma and Mackenzie River basins render it hard to disentangle their sources once stored in lake sediments. On a global scale, but especially in the tropics, brGDGT distributions in lake sediments are substantially different from those in surrounding soils [e.g., *Tierney and Russell*, 2009; *Sinninghe Damsté et al.*, 2009; *Tierney et al.*, 2010; *Loomis et al.*, 2011]. One explanation for the contrasting observation in the Arctic may be the extreme seasonality and short window of biological production at high latitudes, as has indeed been suggested earlier [e.g., *Pearson et al.*, 2011; *Shanahan et al.*, 2013]. Even though it has been shown that seasonality has no effect on brGDGT distributions in temperate soils [*Weijers et al.*, 2011], the results from our study add to a global trend of increasingly contrasting brGDGT distributions between lake sediment and surrounding soil toward the equator and thus with decreasing seasonality and a longer growing season.

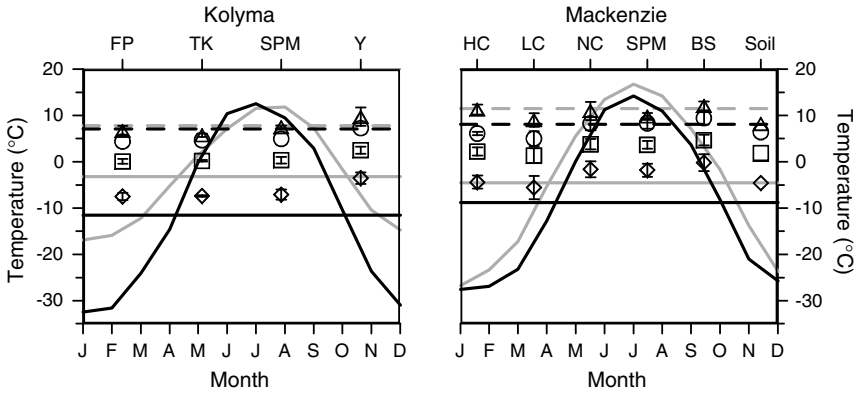

Figure 6. Average brGDGT-based temperatures and standard deviation based on the soil (diamond [*Weijers et al.*, 2007b]; square [*Peterse et al.*, 2012]) and global lake (triangle [*Pearson et al.,* 2011]; circle [*Sun et al.*, 2011]) calibrations compared to the mean annual air temperature variability, MAT (straight line), and SAT (dashed line) in the source (grey) and delta (black) areas in the Kolyma and Mackenzie Rivers.

This suggests that brGDGTs produced in lakes could be more sensitive to seasonal variations than brGDGTs in soils.

For example, the distribution of brGDGTs in and around Lake Cadagno, located at high elevation in the Swiss Alps with a MAT close to 0°C and strong seasonality, are very similar, with average differences in MBT and CBT index values for the lake sediment and the surrounding surface soils of 0.01 and 0.07, respectively [*Niemann et al.*, 2012]. This led the authors to conclude that in situ production was minimal in this lake. Also, a high-altitude lake on the Tibetan Plateau (Lake Qinghai, 3193 m) has a relatively minor sediment-soil offset, i.e., 0.10 for the MBT and 0.12 for the CBT index [*Wang et al.*, 2012]. At a midlatitude site (Sand Pond, Rhode Island, USA), larger average sediment-soil offsets of about 0.3 (MBT) and 0.6 (CBT) are already apparent [*Tierney et al.*, 2012]. Finally, sediment-soil offsets in tropical lake catchments with minor seasonal temperature variation, such as Lake Towuti in Indonesia and Lake Challa in Tanzania, are even larger, averaging about 0.35 and 0.20 for the MBT index and 0.85 for the CBT index [*Sinninghe Damsté et al.*, 2009; *Tierney and Russell*, 2009]. The MBT and CBT index values are systematically higher in the surface soils surrounding the lakes, implying that brGDGT-IIIa and brGDGTs with one cyclopentane moiety (mainly brGDGT-IIb and brGDGT-Ib) are characteristics for brGDGTs of lacustrine origin. Although one study on brGDGTs in soils and lakes along an altitudinal transect in Uganda does not fit the above trend, showing smaller offsets than expected based on its tropical location (MBT offsets are 0.01 and 0.04, and CBT offsets are 0.32 and 0.31 for low- and high-elevation sites, respectively), it does support the increased relative contribution of brGDGTs IIIa, IIb, and Ib in lake sediments [*Loomis et al.*, 2011].

5.4. Applicability of brGDGT-Based Temperature Proxies in Arctic Lakes

Working on the premise that the brGDGT signature in Arctic lake sediments is dominantly of soil origin, we initially calculate MATs using the soil-based MBT-CBT (equation (3)) and MBT′-CBT (equation (5)) transfer functions [*Weijers et al.*, 2007b; *Peterse et al.*, 2012]. Although the MAT in the Mackenzie and Kolyma basins lies outside the temperature range of these soil calibrations, the Weijers et al's. calibration has previously yielded reliable MAT estimates for soils from areas with a MAT as low as −6°C, i.e., Svalbard [*Peterse et al.*, 2009]. Application of this calibration in the Kolyma watershed results in average MATs ranging from −8.6 to −6.4°C for the lakes and −8.9 to −6.1°C for river SPM (Figure 6). These temperatures are a little higher than the measured MAT in the delta (−11.5°C, Cherskiy); however, this is expected as river SPM, and the associated soil-derived brGDGT signature is likely to be sourced from areas of the drainage basin that include warmer regions feeding upstream sections of the river to the south (MAT = −3.2°C, Magadan, near the southernmost portion of the watershed).

The brGDGTs in the Mackenzie River delta lake sediments correspond to a relatively wide range of MATs (−9.5 to 0.4°C using the calibration of *Weijers et al.* [2007b]) and fall within approximately the same range as measured MAT around Great Slave Lake (−4.6°C, Yellowknife) and that in the delta (−8.8°C, Inuvik),

considering the calibration error. The brGDGTs in the NC lakes return higher MAT values than those in the LC and HC lakes (respectively, -1.6 ± 1.8°C versus -5.6 ± 2.5°C and -4.4 ± 1.4°C; Figure 6), which may be due to a larger proportion of soil- or river-derived brGDGTs delivered by the Mackenzie River. However, the ranges of reconstructed temperatures for the different lake types overlap, and average differences are all within the calibration error of the proxy. The MAT of −4.6°C derived from the brGDGTs in the single soil sample analyzed from this region suggests that the MBT-CBT-temperature relation can be extrapolated beyond the minimum temperature of the calibration. The brGDGT distribution in the bank sediments translates to slightly higher temperatures, with values around −1°C in the Mackenzie Delta bank sediments (East, Middle, and Reindeer Channels, Tsiigehtchic, Lake LD-1) and a temperature of 3.5°C for the Peel River. However, the latter drains a different watershed (younger material, more mountainous, and relatively high sediment load [e.g., *Millot et al.*, 2003]) than the Mackenzie, and these differences may be reflected by the brGDGTs. Also, the brGDGTs in the river SPM reflect temperatures that are generally higher than in the delta lakes and increase from −3.2°C under ice to 1.2°C in summer (Figure 6). The higher-than-in-the-delta temperatures fit with a general provenance of the SPM in the relatively warmer lake area upstream the river.

Application of the revised MBT'-CBT calibration (equation (5) [*Peterse et al.*, 2012]) results in MATs for both the Kolyma and the Mackenzie systems that are up to ~8°C higher than those using the original MBT-CBT calibration, although the overall trends remain unchanged (Figure 6). The higher temperatures are likely a consequence of the difference in slope of the revised and original soil calibrations. While the shallower slope of the revised calibration supposedly better tunes the proxy for mid-latitude and lower latitude MAT calculations [e.g., *Peterse et al.*, 2012; *Ernst et al.*, 2013], in return it appears to lead to overestimated MATs at higher latitudes where measured MAT is below the calibrated temperature range. Hence, the original soil calibration seems better suited to generate reliable MAT estimates for Arctic paleotemperature reconstruction.

With the exception of yedoma samples, the brGDGT-derived MATs in the Kolyma basin are all in the same range (Figure 6), supporting the likelihood of a common origin of the brGDGTs in sediments of the FP and TK lakes. In the Mackenzie watershed, however, only MATs derived for the NC lakes resemble those for the SPM and bank sediments, whereas the brGDGTs in the LC and HC lakes reflect lower temperatures (Figure 6). This offset suggests that these lake types must indeed receive additional brGDGTs, which could either originate from local soils with a cooler brGDGT distribution, or from in situ production. Alternatively, the in situ signal in these lakes is less swamped by the SPM contribution in the NC lakes. Since brGDGT concentrations indicate that additional in situ production is likely for all lakes included in this study, global lake-specific temperature calibrations should also generate sensible temperature estimates, as these are designed to correct for any brGDGT production in the water column and/or lake sediments. Unfortunately, MATs obtained when applying the *Sun et al.* [2011] calibration for lakes with pH < 8.5 (equation (6)) overestimate the actual MAT in the Kolyma and Mackenzie catchments. In contrast, the application of the transfer function derived by *Pearson et al.* [2011] (equation (7)), who specifically used summer air temperatures for their calibration, generates temperatures for both river systems that generally reflect those of the summer season (Figure 6 and Table 2). If in situ production of brGDGTs in Arctic lakes primarily takes place during the summer season instead of throughout the whole year, this will likely introduce a warm bias upon the application of transfer functions based on lake data sets in which Arctic lakes are currently underrepresented and calibrated on the annual mean air temperatures. Thus, the contrasting results from both lake calibrations are likely caused by the extreme conditions and seasonal variability in the Arctic.

6. Conclusions

The comparison of brGDGT distributions in thermokarst, floodplain, and deltaic lake sediments, as well as in yedoma permafrost and river SPM in the lower Kolyma and Mackenzie River systems suggests that the majority of brGDGTs in Arctic lake sediments is derived from soils, either indirectly delivered by the river, or directly through thawing permafrost collapse. However, the high brGDGT concentrations in the lake sediments imply either exceptional preservation of the soil-brGDGTs after deposition or additional in situ brGDGT production in lakes. Nevertheless, the limited variability in brGDGT signatures of the different sample sets indicates that even if aquatic brGDGT production is significant, it must yield similar distributions to those in soils. This is likely a consequence of the extreme seasonality and short-growing season at high latitudes.

While MATs in the study areas are below the current calibration range of the brGDGT-based paleotemperature proxies, application of the original MBT-CBT soil calibration [*Weijers et al.*, 2007b] generates MAT estimates that closely resemble measured MAT. The revised MBT'-CBT calibration [*Peterse et al.*, 2012] however results in overestimated MATs, probably due to the more gentle slope of this calibration. Interestingly, the global lake calibration of *Pearson et al.* [2011] also yields reasonable summer air temperatures despite any evidence for significant contribution from in situ-produced brGDGTs. Therefore, our data support the applicability of brGDGT-based paleothermometry in high-latitude lakes provided that the transfer function is selected with care and that potential implications of mixed brGDGT sources are taken into account.

Acknowledgments

We would like to thank the editor and two anonymous reviewers for their constructive comments that have improved the manuscript. We also like to thank M.L. Tavagna and G. Fiske for providing the maps and K.-J. van Groenigen for the help with bootstrapping. R. Macdonald and M. Yunker are thanked for the provision of selected Mackenzie samples and D. Montluçon, V. Galy, and D. Griffith for their assistance with the collection of the Mackenzie lake cores. This work has been supported by an ETH Fellowship (FEL-36 11-1) and NWO Veni grant (863.13.016) to F.P., NWO Rubicon (825.10.022) and Veni (863.12.004) grants to J.E.V., as well as financial support from U.S. NSF (Polaris project 1044610 and Arctic-GRO 0732522 and 1107774), and the WHOI Arctic Research Initiative. All raw data are available through the corresponding author.

References

Bendle, J. A., J. W. H. Weijers, M. A. Maslin, J. S. Sinninghe Damsté, S. Schouten, E. C. Hopmans, C. S. Boot, and R. D. Pancost (2010), Major changes in glacial and Holocene terrestrial temperatures and sources of organic carbon recorded in the Amazon fan by tetraether lipids, *Geochem. Geophys. Geosyst.*, *11*, Q12007, doi:10.1029/2010GC003308.

Birkholz, A., R. H. Smittenberg, I. Hajdas, L. Wacker, and S. M. Bernasconi (2013), Isolation and compound specific radiocarbon dating of terrigenous branched glycerol dialkyl glycerol tetraethers (brGDGTs), *Org. Geochem.*, *60*, 9–19, doi:10.1016/j.orggeochem.2013.04.008.

Blaga, C. I., G.-J. Reichart, S. Schouten, A. F. Lotter, J. P. Werne, S. Kosten, N. Mazzeo, G. Lacerot, and J. S. Sinninghe Damsté (2010), Branched glycerol dialkyl glycerol tetraethers in lake sediments: Can they be used as temperature and pH proxies?, *Org. Geochem.*, *41*, 1225–1234, doi:10.1016/j.orggeochem.2010.07.002.

Callaghan, T. V., F. Bergholm, T. R. Christensen, C. Jonasson, U. Kokfelt, and M. Johansson (2010), A new climate era in the sub-Arctic: Accelerating climate changes and multiple impacts, *Geophys. Res. Lett.* *37*, L14705, doi:10.1029/2009GL042064.

Chylek, P., C. K. Folland, G. Lesins, M. K. Dubey, and M. Wang (2009), Arctic air temperature change amplification and the Atlantic Multidecadal Oscillation, *Geophys. Res. Lett.*, *36*, L14801, doi:10.1029/2009GL038777.

De Jonge, C., A. Stadnitskaia, E. C. Hopmans, G. Cherkashov, A. Fedotov, and J. S. Sinninghe Damsté (2014), In-situ produced branched glycerol dialkyl glycerol tetraethers in suspended particulate matter from the Yenisei River, Eastern Siberia, *Geochim. Cosmochim. Acta*, *125*, 476–491, doi:10.1016/j.gca.2013.10.031.

Dirghangi, S. S., M. Pagani, M. T. Hren, and B. J. Tipple (2013), Distribution of glycerol dialkyl glycerol tetraethers in soils from two environmental transects in the U.S.A., *Org. Geochem.*, *59*, 49–60, doi:10.1016/j.orggeochem.2013.03.009.

Efron, B. (1979), Bootstrap methods: Another look at the jacknife, *Ann. Stat.*, *7*, 1–26, doi:10.1214/aos/1176344552.

Ernst, N., F. Peterse, S. F. M. Breitenbach, H. J. Syiemlieh, and T. I. Eglinton (2013), Biomarkers record environmental changes along an altitudinal transect in the wettest place on Earth, *Org. Geochem.*, *60*, 93–99, doi:10.1016/j.orggeochem.2013.05.004.

Fawcett, P. J., et al. (2011), Extended megadroughts in the southwestern United States during Pleistocene interglacials, *Nature*, *470*, 518–521, doi:10.1038/nature09839.

Gao, L., J. S. Nie, S. Clemens, W. G. Liu, J. M. Sun, R. Zech, and Y. S. Huang (2012), The importance of solar insolation on the temperature variations for the past 110 kyr on the Chinese Loess Plateau, *Palaeogeogr. Palaeoclimatol. Palaeoecol.*, *317*, 128–133, doi:10.1016/j.palaeo.2011.12.021.

Hedges, J. I., W. A. Clark, P. D. Quay, J. E. Richey, A. H. Devol, and U. D. M. Santos (1986), Compositions and fluxes of particulate organic material in the Amazon River, *Limnol. Oceanogr.*, *31*, 717–738.

Holmes, R. M., J. W. McClelland, B. J. Peterson, I. A. Shiklomanov, A. I. Shiklomanov, A. V. Zhulidov, V. V. Gordeev, and N. N. Bobrovitskaya (2002), A circumpolar perspective on fluvial sediment flux to the Arctic Ocean, *Global Biogeochem. Cycles*, *16*(4), 1098, doi:10.1029/2001GB001849.

Holmes, R. M., et al. (2012), Seasonal and Annual Fluxes of Nutrients and Organic Matter from Large Rivers to the Arctic Ocean and Surrounding Seas, *Estuar. Coast.*, *35*, 369–382, doi:10.1007/s12237-011-9386-6.

Hopmans, E. C., J. W. H. Weijers, E. Schefuss, L. Herfort, J. S. Sinninghe Damsté, and S. Schouten (2004), A novel proxy for terrestrial organic matter in sediments based on branched and isoprenoid tetraether lipids, *Earth Planet. Sci. Lett.*, *224*, 107–116, doi:10.1016/j.epsl.2004.05.012.

Hren, M. T., M. Pagani, D. M. Erwin, and M. Brandon (2010), Biomarker reconstruction of the early Eocene paleotopography and paleoclimate of the northern Sierra Nevada, *Geology*, *38*, 7–10, doi:10.1130/G30215.1.

Huguet, C., E. C. Hopmans, W. Febo-Ayala, D. H. Thompson, J. S. Sinninghe Damsté, and S. Schouten (2006), An improved method to determine the absolute abundance of glycerol dibiphytanyl glycerol tetraether lipids, *Org. Geochem.*, *37*, 1036–1041, doi:10.1016/j.orggeochem.2006.05.008.

Kim, J.-H., C. Zell, P. Moreira-Turcq, M. A. P. Pérez, G. Abril, J.-M. Mortillaro, J. W. H. Weijers, T. Meziane, and J. S. Sinninghe Damsté (2012), Tracing soil organic carbon in the lower Amazon River and its tributaries using GDGT distributions and bulk organic matter properties, *Geochim. Cosmochim. Acta*, *90*, 163–180, doi:10.1016/j.gca.2012.05.014.

Liu, X.-L., A. Leider, A. Gillespie, J. Groeger, G. J. M. Versteegh, and K.-U. Hinrichs (2010), Identification of polar lipid precursors of the ubiquitous branched GDGT orphan lipids in a peat bog in Northern Germany, *Org. Geochem.*, *41*, 653–660, doi:10.1016/j.orggeochem.2010.04.004.

Lobbes, J. M., H. P. Fitznar, and G. Kattner (2000), Biogeochemical characteristics of dissolved and particulate organic matter in Russian rivers entering the Arctic Ocean, *Geochim. Cosmochim. Acta*, *64*, 2973–2983, doi:10.1016/S0016-7037(00)00409-9.

Loomis, S. E., J. M. Russell, and J. S. Sinninghe Damsté (2011), Distributions of branched GDGTs in soils and lake sediments from western Uganda: Implications for a lacustrine paleothermometer, *Org. Geochem.*, *42*, 739–751, doi:10.1016/j.orggeochem.2011.06.004.

Loomis, S. E., J. M. Russell, B. Ladd, F. A. Street-Perrott, and J. S. Sinninghe Damsté (2012), Calibration and application of the branched GDGT temperature proxy on East African lake sediments, *Earth Planet. Sci. Lett.*, *357*, 277–288, doi:10.1016/j.epsl.2012.09.031.

Macdonald, R. W., K. Iseki, M. C. O'Brien, F. A. McLaughlin, S. McCullough, D. M. Macdonald, E. C. Carmack, M. Yunker, S. Buckingham, and G. Miskulin (1988), NOGAP B.6; Volume 5: Chemical data collected in the Beaufort Sea and Mackenzie River delta March-July 1987, *Canadian Data Report of Hydrography and Ocean Sciences* No. 60. 56 pp.

Marsh, P., and M. Hey (1989), The flooding hydrology of Mackenzie Delta Lakes near Inuvik, N.W.T., Canada, *Arctic*, *42*, 41–49.

McGuire, A. D., L. G. Anderson, T. R. Christensen, D. Scott, G. Laodong, D. J. Hayes, H. Martin, T. D. Lorenson, R. W. Macdonald, and R. Nigel (2009), Sensitivity of the carbon cycle in the Arctic to climate change, *Ecol. Monogr.*, *79*, 523–555, doi:10.1890/08-2025.1.

Millot, R., J. Gaillardet, B. Dupré, and C. J. Allègre (2003), Northern latitude chemical weathering rates: Clues from the Mackenzie River Basin, Canada, *Geochim. Cosmochim. Acta*, *67*, 1305–1329, doi:10.1016/S0016-7037(02)01207-3.

Naeher, S., F. Peterse, R. H. Smittenberg, H. Niemann, P. Zigah, and C. J. Schubert (2014), Sources of glycerol dialkyl glycerol tetraethers (GDGTs) in catchment soils, water column and sediments of Lake Rotsee (Switzerland) - Implications for the application of GDGT-based proxies for lakes, *Org. Geochem.*, *66*, 164–173, doi:10.1016/j.orggeochem.2013.10.017.

Niemann, H., A. Stadnitskaia, S. B. Wirth, A. Gilli, F. S. Anselmetti, J. S. Sinninghe Damsté, S. Schouten, E. C. Hopmans, and M. F. Lehmann (2012), Bacterial GDGTs in Holocene sediments and catchment soils of a high Alpine lake: application of the MBT/CBT-paleothermometer, *Clim. Past*, *8*, 889–906, doi:10.5194/cp-8-889-2012.

Overpeck, J., et al. (1997), Arctic environmental change of the last four centuries, *Science*, *278*, 1251–1256, doi:10.1126/science.278.5341.1251.

Pearson, E. J., S. Juggins, H. M. Talbot, J. Weckstrom, P. Rosen, D. B. Ryves, S. J. Roberts, and R. Schmidt (2011), A lacustrine GDGT-temperature calibration from the Scandinavian Arctic to Antarctic: Renewed potential for the application of GDGT-paleothermometry in lakes, *Geochim. Cosmochim. Acta*, *75*, 6225–6238, doi:10.1016/j.gca.2011.07.042.

Peterse, F., J.-H. Kim, S. Schouten, D. Klitgaard Kristensen, N. Koç, and J. S. Sinninghe Damsté (2009), Constraints on the application of the MBT/CBT palaeothermometer at high latitude environments (Svalbard, Norway), *Org. Geochem.*, *40*, 692–699, doi:10.1016/j.orggeochem.2009.03.004.

Peterse, F., E. C. Hopmans, S. Schouten, A. Mets, W. I. C. Rijpstra, and J. S. Sinninghe Damsté (2011a), Identification and distribution of intact polar branched tetraether lipids in peat and soil, *Org. Geochem.*, *42*, 1007–1015, doi:10.1016/j.orggeochem.2011.07.006.

Peterse, F., M. A. Prins, C. J. Beets, S. R. Troelstra, H. Zheng, Z. Gu, S. Schouten, and J. S. Sinninghe Damsté (2011b), Decoupled warming and monsoon precipitation in East Asia over the last deglaciation, *Earth Planet. Sci. Lett.*, *301*, 256–264, doi:10.1016/j.epsl.2010.11.010.

Peterse, F., J. van der Meer, S. Schouten, J. W. H. Weijers, N. Fierer, R. B. Jackson, J.-H. Kim, and J. S. Sinninghe Damsté (2012), Revised calibration of the MBT-CBT paleotemperature proxy based on branched tetraether membrane lipids in surface soils, *Geochim. Cosmochim. Acta*, *96*, 215–229, doi:10.1016/j.gca.2012.08.011.

Richter-Menge, J., M. O. Jeffries, and J. E. Overland (2011). Arctic Report Card 2011. [Available at http://www.arctic.noaa.gov/reportcard.]

Rueda, G., A. Rosell-Mele, M. Escala, R. Gyllencreutz, and J. Backman (2009), Comparison of instrumental and GDGT-based estimates of sea surface and air temperatures from the Skagerrak, *Org. Geochem.*, *40*, 287–291, doi:10.1016/j.orggeochem.2008.10.012.

Schaefer, K., T. Zhang, L. Bruhwiler, and A. P. Barrett (2011), Amount and timing of permafrost carbon release in response to climate warming, *Tellus B Chem. Phys. Meteorol.*, *63*, 165–180, doi:10.1111/j.1600-0889.2011.00527.x.

Schirrmeister, L., V. Kunitsky, G. Grosse, S. Wetterich, H. Meyer, G. Schwamborn, O. Babiy, A. Derevyagin, and C. Siegert (2011), Sedimentary characteristics and origin of the Late Pleistocene Ice Complex on north-east Siberian Arctic coastal lowlands and islands - A review, *Quaternary Int.*, *241*, 3–25, doi:10.1016/j.quaint.2010.04.004.

Schoon, P. L., A. de Kluijver, J. J. Middelburg, J. A. Downing, J. S. Sinninghe Damsté, and S. Schouten (2013), Influence of lake water pH and alkalinity on the distribution of core and intact polar branched glycerol dialkyl glycerol tetraethers (GDGTs) in lakes, *Org. Geochem.*, *60*, 72–82, doi:10.1016/j.orggeochem.2013.04.015.

Schouten, S., C. Huguet, E. C. Hopmans, M. V. M. Kienhuis, and J. S. Sinninghe Damsté (2007), Analytical methodology for TEX86 paleothermometry by high-performance liquid chromatography/atmospheric pressure chemical ionization-mass spectrometry, *Anal. Chem.*, *79*, 2940–2944, doi:10.1021/ac062339v.

Schouten, S., E. C. Hopmans, and J. S. Sinninghe Damsté (2013), The organic geochemistry of glycerol dialkyl glycerol tetraether lipids: A review, *Org. Geochem.*, *54*, 19–61, doi:10.1016/j.orggeochem.2012.09.006.

Shanahan, T. M., K. A. Hughen, and B. A. S. Van Mooy (2013), Temperature sensitivity of branched and isoprenoid GDGTs in Arctic lakes, *Org. Geochem.*, *64*, 119–128, doi:10.1016/j.orggeochem.2013.09.010.

Sinninghe Damsté, J. S., J. Ossebaar, B. Abbas, S. Schouten, and D. Verschuren (2009), Fluxes and distribution of tetraether lipids in an equatorial African lake: Constraints on the application of the TEX(86) palaeothermometer and BIT index in lacustrine settings, *Geochim. Cosmochim. Acta*, *73*, 4232–4249, doi:10.1016/j.gca.2009.04.022.

Sinninghe Damsté, J. S., J. Ossebaar, S. Schouten, and D. Verschuren (2012a), Distribution of tetraether lipids in the 25-ka sedimentary record of Lake Challa: extracting reliable TEX86 and MBT/CBT palaeotemperatures from an equatorial African lake, *Quaternary Sci. Rev.*, *50*, 43–54, doi:10.1016/j.quascirev.2012.07.001.

Sinninghe Damsté, J. S., W. I. C. Rijpstra, E. C. Hopmans, M. Y. Jung, J. G. Kim, S. K. Rhee, M. Stieglmeier, and C. Schleper (2012b), Intact polar and core glycerol dibiphytanyl glycerol tetraether lipids of group I.1a and I.1b Thaumarchaeota in soil, *Appl. Environ. Microbiol.*, *78*, 6866–6874, doi:10.1128/AEM.01681-12.

Sun, Q., G. Chu, M. Liu, M. Xie, S. Li, Y. Ling, X. Wang, L. Shi, G. Jia, and H. Lue (2011), Distributions and temperature dependence of branched glycerol dialkyl glycerol tetraethers in recent lacustrine sediments from China and Nepal, *J. Geophys. Res.*, *116*, G01008, doi:10.1029/2010JG001365.

Tank, S. E., L. F. W. Lesack, J. A. L. Gareis, C. L. Osburn, and R. H. Hesslein (2011), Multiple tracers demonstrate distinct sources of dissolved organic matter to lakes of the Mackenzie Delta, Western Canadian Arctic, *Limnol. Oceanogr.*, *56*, 1297–1309, doi:10.4319/lo.2011.56.4.1297.

Tarnocai, C., J. G. Canadell, E. A. G. Schuur, P. Kuhry, G. Mazhitova, and S. Zimov (2009), Soil organic carbon pools in the northern circumpolar permafrost region, *Global Biogeochem. Cycles*, *23*, GB2023, doi:10.1029/2008GB003327.

Tierney, J. E., and J. M. Russell (2009), Distributions of branched GDGTs in a tropical lake system: Implications for lacustrine application of the MBT/CBT paleoproxy, *Org. Geochem.*, *40*, 1032–1036, doi:10.1016/j.orggeochem.2009.04.014.

Tierney, J. E., J. M. Russell, H. Eggermont, E. C. Hopmans, D. Verschuren, and J. S. Sinninghe Damsté (2010), Environmental controls on branched tetraether lipid distributions in tropical East African lake sediments, *Geochim. Cosmochim. Acta*, *74*, 4902–4918, doi:10.1016/j.gca.2010.06.002.

Tierney, J. E., S. Schouten, A. Pitcher, E. C. Hopmans, and J. S. Sinninghe Damsté (2012), Core and intact polar glycerol dialkyl glycerol tetraethers (GDGTs) in Sand Pond, Warwick, Rhode Island (USA): Insights into the origin of lacustrine GDGTs, *Geochim. Cosmochim. Acta*, *77*, 561–581, doi:10.1016/j.gca.2011.10.018.

van Dongen, B. E., I. Semiletov, J. W. H. Weijers, and Ö. Gustafsson (2008), Contrasting lipid biomarker composition of terrestial organic matter exported from across the Eurasian Arctic by the five great Russian Arctic rivers, *Global Biogeochem. Cycles*, *22*, GB1011, doi:10.1029/2007GB002974.

Vasil'chuk, Y. K., and A. C. Vasil'chuk (1997), Radiocarbon dating and oxygen isotope variations in late Pleistocene syngenetic ice-wedges, Northern Siberia, *Permafrost Periglac. Process.*, *8*, 335–345, doi:10.1002/(SICI)1099-1530(199709)8:3<335::AID-PPP259>3.0.CO;2-V.

Vonk, J. E., et al. (2013), High biolability of ancient permafrost carbon upon thaw, *Geophys. Res. Lett.*, *40*, 2689–2693, doi:10.1002/grl.50348.

Wang, H., W. Liu, C. L. Zhang, Z. Wang, J. Wang, Z. Liu, and H. Dong (2012), Distribution of glycerol dialkyl glycerol tetraethers in surface sediments of Lake Qinghai and surrounding soil, *Org. Geochem.*, *47*, 78–87, doi:10.1016/j.orggeochem.2012.03.008.

Weijers, J. W. H., S. Schouten, O. C. Spaargaren, and J. S. Sinninghe Damsté (2006), Occurrence and distribution of tetraether membrane lipids in soils: Implications for the use of the TEX(86) proxy and the BIT index, *Org. Geochem.*, *37*, 1680–1693, doi:10.1016/j.orggeochem.2006.07.018.

Weijers, J. W. H., E. Schefuss, S. Schouten, and J. S. Sinninghe Damsté (2007a), Coupled thermal and hydrological evolution of tropical Africa over the last deglaciation, *Science*, *315*, 1701–1704, doi:10.1126/science.1138131.

Weijers, J. W. H., S. Schouten, J. C. van den Donker, E. C. Hopmans, and J. S. Sinninghe Damsté (2007b), Environmental controls on bacterial tetraether membrane lipid distribution in soils, *Geochim. Cosmochim. Acta*, *71*, 703–713, doi:10.1016/j.gca.2006.10.003.

Weijers, J. W. H., E. Panoto, J. van Bleijswijk, S. Schouten, W. I. C. Rijpstra, M. Balk, A. J. M. Stams, and J. S. Sinninghe Damsté (2009), Constraints on the biological source(s) of the orphan branched tetraether membrane lipids, *Geomicrobiol. J.*, *26*, 402–414, doi:10.1080/01490450902937293.

Weijers, J. W. H., B. Bernhardt, F. Peterse, J. P. Werne, J. A. J. Dungait, S. Schouten, and J. S. Sinninghe Damsté (2011), Absence of seasonal patterns in MBT-CBT indices in mid-latitude soils, *Geochim. Cosmochim. Acta*, *75*, 3179–3190, doi:10.1016/j.gca.2011.03.015.

Zell, C., J.-H. Kim, P. Moreira-Turcq, G. Abril, E. C. Hopmans, M.-P. Bonnet, R. Lima Sobrinho, and J. S. Sinninghe Damsté (2013), Distentangling the origins of branched tetraether lipids and crenarchaeol in the lower Amazon River: Implications for GDGT-based proxies, *Limnol. Oceanogr.*, *58*, 343–353, doi:10.4319/lo.2013.58.1.0343.

Zimov, S. A., A. P. Davydov, G. M. Zimova, A. I. Davydova, E. A. G. Schuur, K. Dutta, and F. S. Chapin (2006a), Permafrost carbon: Stock and decomposability of a globally significant carbon pool, *Geophys. Res. Lett.*, *33*, L20502, doi:10.1029/2006GL027484.

Zimov, S. A., E. A. G. Schuur, and R. Stuart Chapin III (2006b), Permafrost and the global carbon budget, *Science*, *312*, 1612–1613, doi:10.1126/science.1128908.